

# A novel multi-threshold coupling InAlN/GaN double-channel HEMT for improving transconductance flatness

Sirui AN<sup>1</sup>, Minhan MI<sup>1\*</sup>, Pengfei WANG<sup>1</sup>, Sijia LIU<sup>2</sup>, Qing ZHU<sup>1</sup>, Meng ZHANG<sup>1</sup>,  
Zhihong CHEN<sup>1</sup>, Jielong LIU<sup>3</sup>, Siyin GUO<sup>1</sup>, Can GONG<sup>1</sup>,  
Xiaohua MA<sup>1</sup> & Yue HAO<sup>1</sup>

<sup>1</sup>School of Microelectronics, Xidian University, Xi'an 710071, China;

<sup>2</sup>School of Advanced Materials and Nanotechnology, Xidian University, Xi'an 710071, China;

<sup>3</sup>Hubei Jiufengshan Laboratory, Wuhan 430040, China

Received 6 July 2022/Revised 22 October 2022/Accepted 13 March 2023/Published online 19 December 2023

GaN-based HEMTs have significant advantages, making them a prime choice for high-frequency, high-power switching [1]. However, the inherent poor linearity of GaN HEMT has yet to be solved, which can be reflected by the nonlinearity of the transconductance ( $G_m$ ) profile [2]. This makes it hard to achieve high data transmission efficiency and less signal distortion in the wireless communication system [3].

It is known that the  $G_m$  profile of the DC (double channel) HEMTs owes double  $G_{m\text{-max}}$  features, demonstrating that it is possible to realize  $G_m$  flatter in a wide gate voltage ( $V_{gs}$ ) range [4]. However, the thickness of barriers ( $T_{bar}$ ) and channel-to-channel distance ( $d_{c-c}$ ) is too large to form a close coupling between the channels of the device, making the difference between the peaks so large that limits the transconductance flatness.

In this study, a novel multi-threshold coupling InAlN/GaN DC HEMT (MC-DC HEMT) has been proposed. The fabricated device shows the gate voltage swing (GVS) amplitude of 7.8 V and  $G_{m\text{-max}}$  of 216.3 mS/mm. Also, the current gain cutoff frequency ( $f_T$ ) and maximum oscillation frequency ( $f_{max}$ ) keep constant 34 and 72 GHz in a wider gate voltage bias, and an exceptional linearity performance with the (output third-order intercept point) OIP<sub>3</sub> of 38 dBm, an improvement of 10 dBm compared with the reference device.

**Experiment.** The structure of the MC-DC HEMT investigated is shown in Figures 1(a)–(d). The InAlN DC structure whose  $T_{bar}$  is 8 nm and  $d_{c-c}$  is 18 nm was grown on SiC substrate. For the details of device fabrication see Appendix A.

**Result and discussion.** The optimal structural parameters of the MC-DC HEMT (see Appendixes B and C) are  $W_R = 0.2 \mu\text{m}$ ,  $H_R = 18 \text{ nm}$ , and  $\alpha = 0.8$ .

Figure 1(h) demonstrates that the  $G_{m\text{-max}}$  of the MC-DC HEMT, compared with that of planar HEMT, is reduced. But GVS reaches a maximum amplitude of 7.8 V. And the

threshold voltage ( $V_{th}$ ) drifted positive to  $-9.3 \text{ V}$ , and the maximum drain current density ( $I_{d\text{-max}}$ ) is 1622 mA/mm, as shown in Figure 1(i). It is known that when the power amplifier enlarges an input signal of frequency  $f$ , the base wave output signal and  $G_m$  are positively correlated, while the harmonic outputs at frequencies  $2f$  and  $3f$  are also positively correlated with the first and second-order derivatives of  $G_m$  [2]. Figures 1(j) and (k) show that the derivatives of  $G_m$  of the MC-DC HEMT improve slightly in the transition region from the subthreshold to the peak value. In the linear increase region, the  $G_m$  profile of the MC-DC HEMT is much flatter, thus suppressing the undesired harmonic component. The results show that the MC structure effectively improves the transconductance flatness, and Figure 1(l) shows its advantage in device-level linearization technology.

To characterize the small-signal performance of the MC-DC HEMT. As shown in Figures 1(m)–(o), the maximum  $f_T/f_{max}$  for MC-DC HEMTs is 34/72 GHz, and also,  $f_T$  and  $f_{max}$  maintain constant over a very wide gate voltage range of GVS over 7 V.

The two-tone characteristic of the MC-DC HEMT of OIP<sub>3</sub> is 38 dBm, corresponding to the input third-order intercept point (IIP<sub>3</sub>) of 27 dBm. This result shows a good agreement with the flatter  $G_m$  curve, and the  $G'_m$ ,  $G''_m$  of the MC-DC HEMT are closer to zero over a wide range of  $V_{gs}$ , effectively suppressing harmonics and OIP<sub>3</sub> degradation, making MC-DC HEMT a competitive candidate in realizing high linearity at high power conditions.

**Conclusion.** This work proposed an InAlN/GaN MC-DC HEMT, with a selective-etched upper barrier and a complete non-etched lower channel to improve  $G_m$  flatness. The device has excellent  $G_m$  flatness in DC performance as GVS close to 8 V, nearly constant  $f_T$  and  $f_{max}$  profiles, and OIP<sub>3</sub> improved by 10 dBm compared with the reference device.

\* Corresponding author (email: miminhan@qq.com)

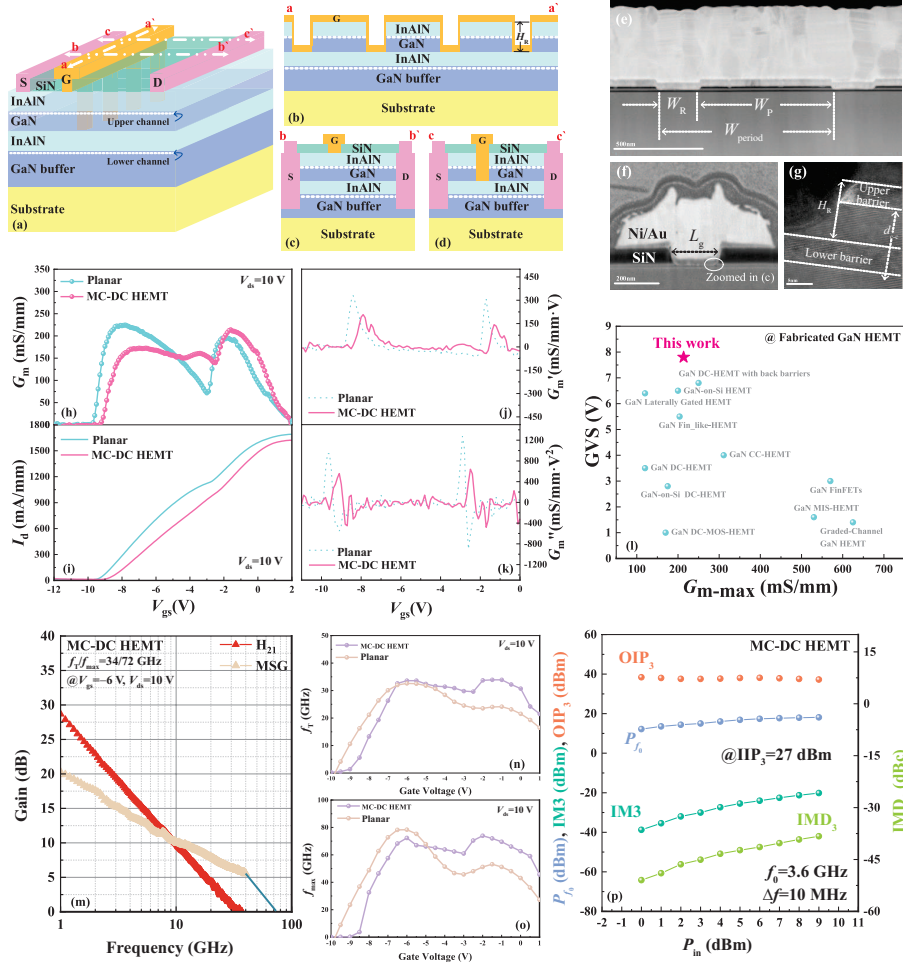


**Figure 1** (Color online) (a) Structure diagram of the novel InAlN/GaN MC-DC HEMT cross-sectional views of the MC-DC HEMT (b) along the gate width, (c) planar region and (d) recess region along the source-drain direction; (e) SEM view of the cross-section along the gate width, the width of the recess region ( $W_R$ ), and the proportion of the width of the planar region ( $W_P$ ) to a period width ( $W_{\text{period}}$ ) called the etching ratio ( $\alpha$ ), where  $W_{\text{period}} = 1 \mu\text{m}$ ,  $W_P = 800 \text{ nm}$ ,  $W_R = 200 \text{ nm}$ ,  $\alpha = W_P/W_{\text{period}} = 0.8$ ; (f) SEM view of the cross section at recess region along the gate length; SEM view of the oval-shaped in (f) zoomed in (g); the etching recess depth ( $H_R$ ) is defined as the downward etching distance of the upper barrier surface, where  $H_R = 18 \text{ nm}$ ; the MC-DC HEMT at  $W_R = 200 \text{ nm}$ ,  $H_R = 18 \text{ nm}$ ,  $\alpha = 0.8$  comparison of (h)  $G_m$  profile and (i) transfer characteristics; (j) the first- and (k) second-order derivatives of  $G_m$  profiles of HEMT; (l) benchmark of reported GaN-based HEMTs in terms of GVS versus  $G_{m\text{-max}}$ ; (m) small-signal characteristics of MC-DC HEMTs, (n)  $f_T$  and (o)  $f_{\text{max}}$  versus  $V_{\text{gs}}$ ; (p) two-tone power linearity measurements at 3.6 GHz with tone spacing of 10 MHz for MC-DC HEMT.

This impressive improvement in  $G_m$ , small- and large-signal linearity indicates that the novel MC-DC HEMT provides an approach to be used in high-linearity RF applications.

**Acknowledgements** This work was supported by National Key R&D Program of China (Grant No. 2021YFB3602404).

**Supporting information** Appendixes A–E. The supporting information is available online at [info.scichina.com](http://info.scichina.com) and [link.springer.com](http://link.springer.com). The supporting materials are published as submitted, without typesetting or editing. The responsibility for scientific accuracy and content remains entirely with the authors.

## References

- Nagy W, Brown J, Borges R, et al. Linearity characteristics of microwave-power GaN HEMTs. *IEEE Trans Microwave Theor Techn*, 2003, 51: 660–664
- Joglekar S, Radhakrishna U, Piedra D, et al. Large signal linearity enhancement of AlGaIn/GaN high electron mobility transistors by device-level  $V_t$  engineering for transconductance compensation. In: *Proceedings of IEEE International Electron Devices Meeting (IEDM)*, San Francisco, 2017
- Moon J, Grabar B, Wong J, et al. Ultra-linear and high-efficiency GaN technology for 5G and beyond. In: *Proceedings of IEEE Topical Conference on RF/Microwave Power Amplifiers for Radio and Wireless Applications (PAWR)*, 2022. 5–7
- Song W J, Zheng Z, Chen T, et al. RF linearity enhancement of GaN-on-Si HEMTs with a closely coupled double-channel structure. *IEEE Electron Device Lett*, 2021, 42: 1116–1119